Supporting Information for

Development of deep-blue exciplex as emitter and host for highly efficient and wide-color OLEDs

Qing Xia[#] ,Yuhao Xiang[#], Yujie Gong, Shuai Li, Yishi Wu, Zhijia Wang, Hongbing Fu[*]

 Beijing Key Laboratory for Optical Materials and Photonic Devices, Department of Chemistry, Capital Normal University, Beijing 100048, P. R. China.

E-mail: hbfu@cnu.edu.cn

#Q. X. and Y. X. contributed equally to this work.

Keywords: deep-blue exciplex emission, thermally activated delayed fluorescence, organic light-emitting diode, energy transfer, phosphorescence

A. Experimental Details.

Synthesis of (Z)-3-(diphenylamino)-3-hydroxy-N,N-diphenylacrylamide (DNPhDCO):
Diphenylamine (1.015 g, 6 mmol) and 30 mL dry tetrahydrofuran (THF) were added into a 50 mL
two neck flask. Under nitrogen atmosphere, 0.3 mL malonyl dichloride (3 mmol) was added
slowly. The reaction was then stirred at room temperature for 1 hour. Then, the reaction solution
was concentrated under reduced pressure. The crude product was recrystallization from ethanol to
afford DNPhDCO as white solid (0.89 g, 72%).

*Synthesis of Difluoroboron (Z)-3-(diphenylamino)-3-hydroxy-N,N-diphenylacrylamide
(DNPhB)*: Compound DNPhDCO (813 mg, 2 mmol) was dissolved in 30 mL of dry CH_2Cl_2. Under
nitrogen atmosphere, BF_3.Et_2O (760 μL, 6 mmol) solution was added. The reaction mixture was
stirred at room temperature overnight in the dark. Then add ethanol to the solution, Then, the
reaction solution was concentrated under reduced pressure. The crude product was recrystallization
from ethanol to afford DNPhB as white solid (0.835g, 66%). ^{1}H NMR (400 MHz, d-DMSO, ppm):
δ= 7.40 (t, J = 16 Hz, 8*H*), 7.35-7.27 (m, 12*H*), 4.03 (s, 1*H*).^{13}C NMR (151 MHz, $CDCl_3$) δ 167.6,
141.2, 129.3, 127.3, 127.2, 71.3.

Instruments: ^{1}H NMR, ^{13}C NMR spectra were recorded on a Bruker ADVANCE-400 fourier
transformation spectrometer. The spectra were calibrated with respect to the residual solvent peaks.
The chemical shifts are reported in parts per millon (ppm) with respect to TMS. Short notations
used are, s for singlet, d for doublet, t for triplet, q for quartet and m for multiplet.
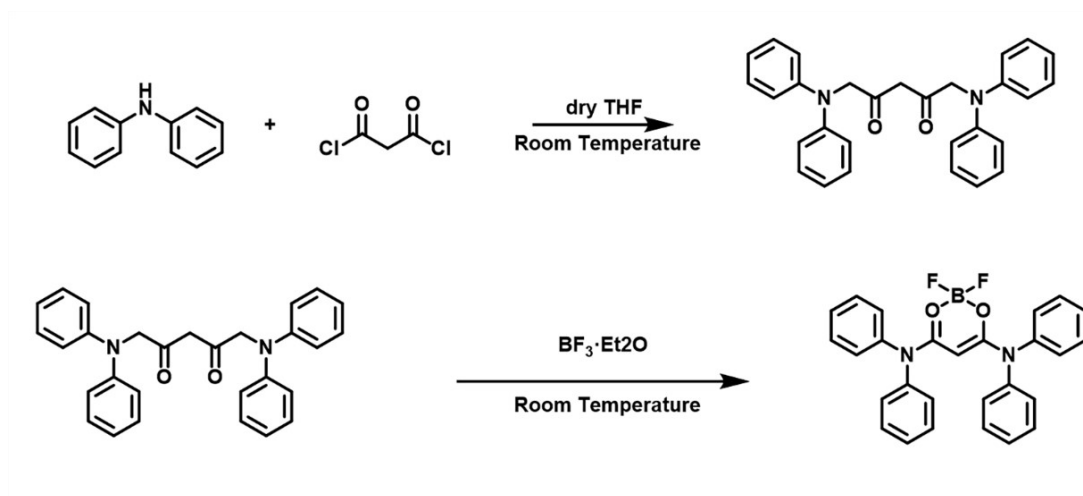
Scheme S1. The synthetic route of compound DNPhB.
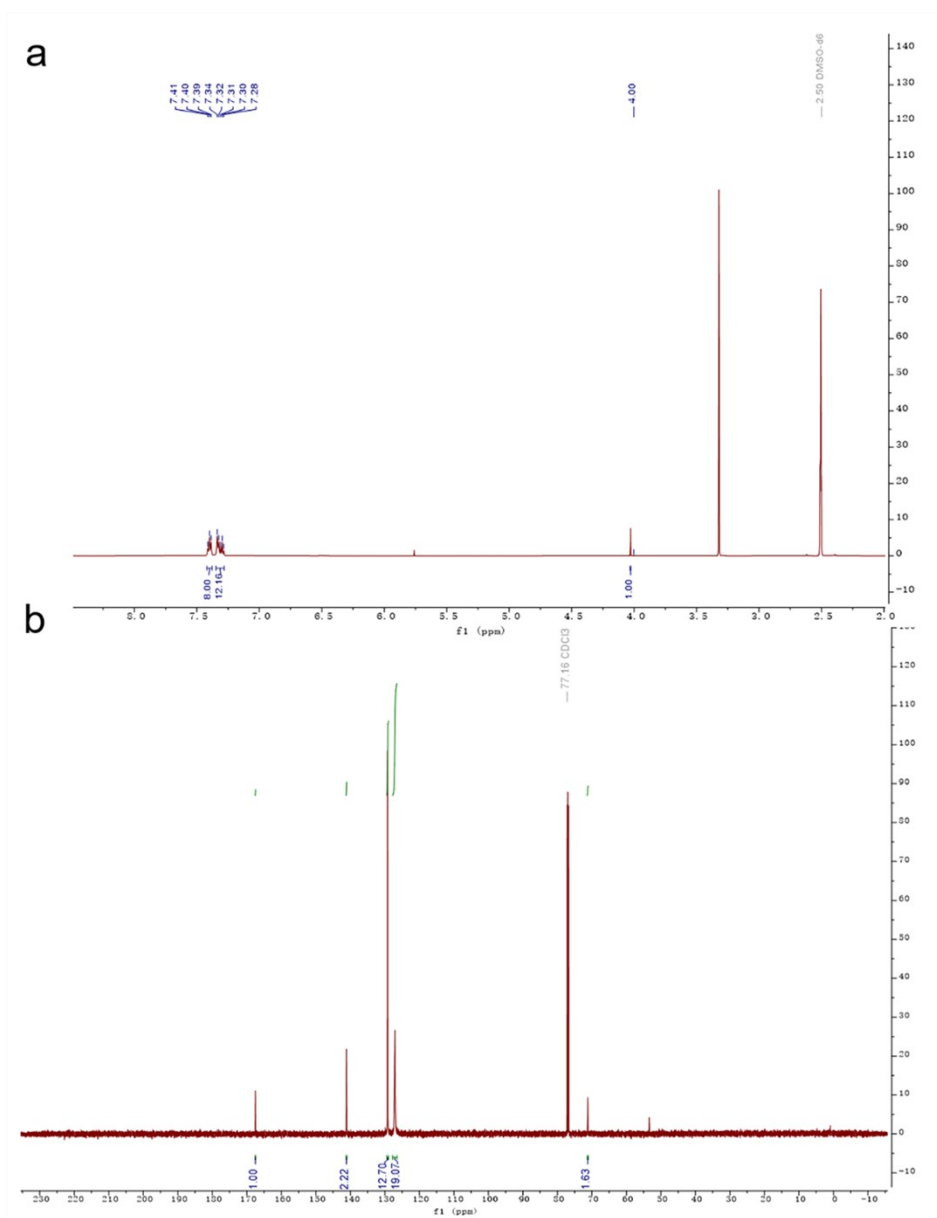
Fig. S1 (a) ^{1}H NMR spectrum of DNPhB in *d*-DMSO, (b) ^{13}C NMR spectrum of DNPhB in CDCl$_3$.

Ultraviolet Photo-electron Spectroscopy measurements (UPS):

UPS measurements were conducted with a Kratos Axis Ultra [DLD] spectrometer (Kratos, Manchester, England). During UPS measurement, the sample was held at a bias of -9 V with respect to the spectrometer. Illumination at 21.22 eV was provided by the He(I) emission line from a helium discharge lamp.
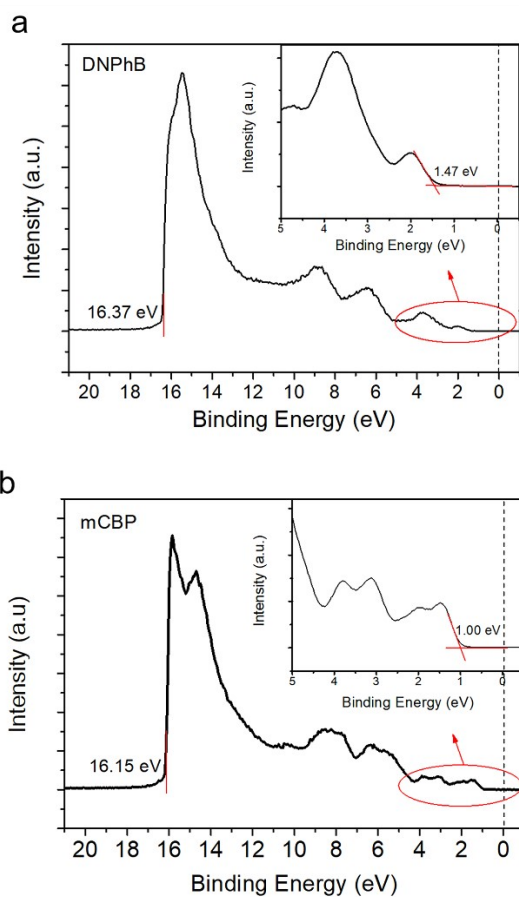
Fig. S2 Ultraviolet photoelectron spectroscopy (UPS) of (a) mCBP, (b) DNPhB.

Table S1. The data of HOMO/LUMO of mCBP and DNPhB in neat films.

Sample	HOMO[a] (eV)	LUMO[b] (eV)
DNPhB	-6.32	-2.90
mCBP	-6.07	-2.59

[a] Measured in ultraviolet photoelectron spectroscopy (UPS) at the same time; [b] Calculated from λ_{onset}.

Theoretical calculations

All the density functional theory (DFT) calculations are performed using Gaussion 09 software package with B3LYP functional and 6-31G(d) basis set.

LUMO: -2.37eV

Gap: 3.56 eV

HOMO: -5.93eV
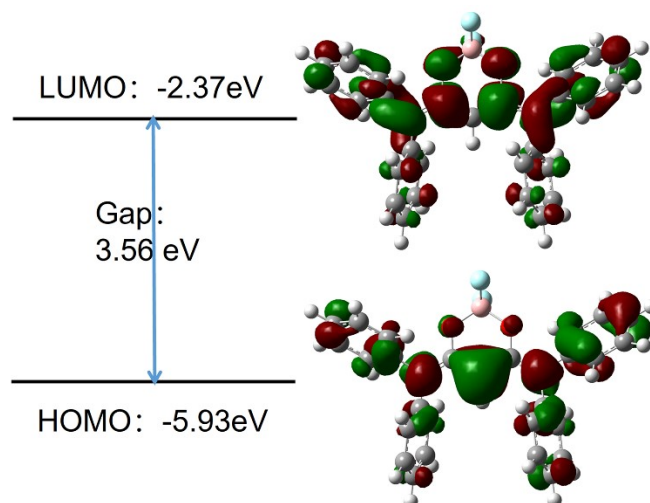
Fig. S3 Optimized geometry and molecular orbitals of DNPhB

Table S2. Calculated emission wavelength, oscillator strength (f) and HOMO/LUMO level for DNPhB at the B3LYP/ 6-31G(d) level.

Structure	λ_{abs} (nm)	λ_{PL} (nm)	HOMO (eV)	LUMO (eV)
DNPhB	315	496	-5.93	-2.37
	f= 0.9079	f= 0.3500		

Photophysical Property Measurements:

The UV-visible absorption spectra were measured on a Hitachi UV-U3900H spectrometer with a slit width of 1 nm. The photoluminescence (PL) spectra were measured on a Hitachi F-4600 and Edinburgh FLS 1000 fluorescence spectrophotometer. The fluorescence lifetime and time-resolved emission spectrum detected with a streak camera (C10647, Hamamatsu Photonics) upon 400 nm femtosecond laser excitation. The temperature-dependent lifetime decay profiles were measured using a closed cycle cryostat (oxford-instruments Optistat DN). The phosphorescence spectrum was obtained using an Edinburgh FLS 1000 fluorescence spectrophotometer at 77 K in a dewar vessel with 1 ms delay time after excitation using a microsecond (μs) flash lamp.
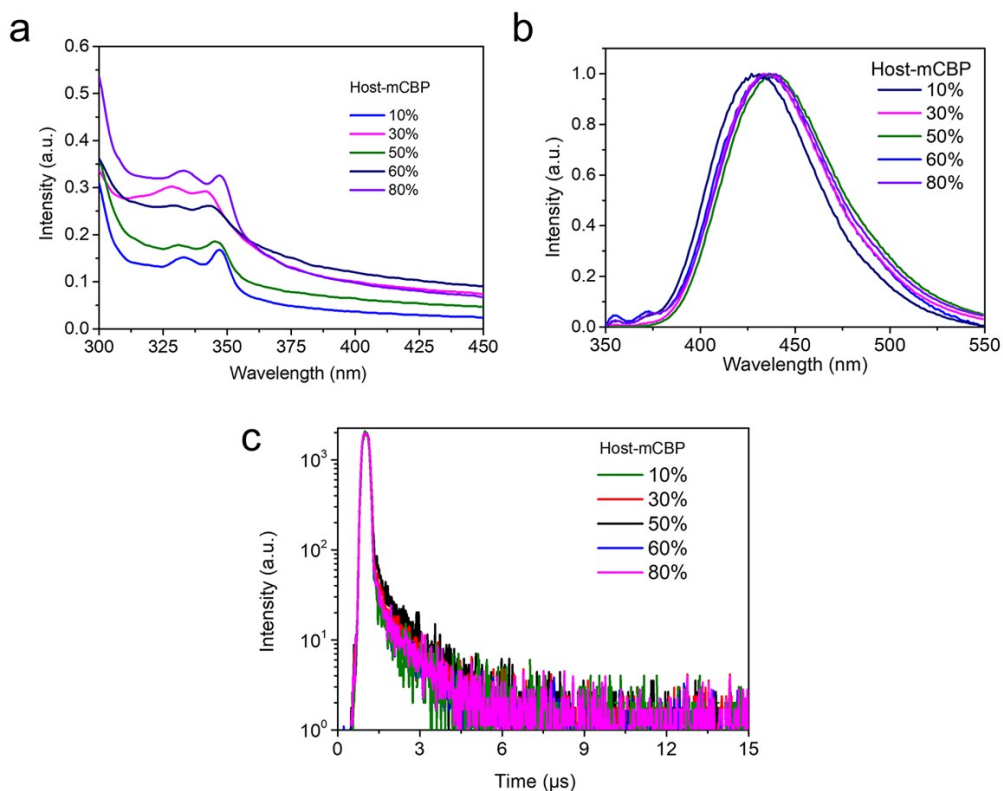
Fig. S4 (a) UV-Vis absorption (b) fluorescence spectra and (c) PL transient decay spectra at room temperature for DNPhB-doped films of mCBP with different doped ratio.

Table S3. the data of DNPhB (X%) blend films doped with mCBP (1-X%).

X	λ_{abs}[a]	λ_{PL}[b]	FHWH	Φ_{PL}[c]	τ_d[d]
(%)	(nm)	(nm)	(nm)	(%)	(µs)
10	331, 342	420	71	39	0.95
30	331, 342	433	70	50.8	0.98
50	331, 342	444	73	56.1	1.01
60	331, 342	437	71	53.6	0.96
80	331, 344	435	70	45.5	0.96

[a] Absorption measured in 10^{-5} mol L^{-1} polystyrene solution; [b] Steady-state PL at room temperature measured in films. [c] PL quantum yield measured in films using an integral sphere. [d] Lifetime of fluorescence determined from the transient PL.
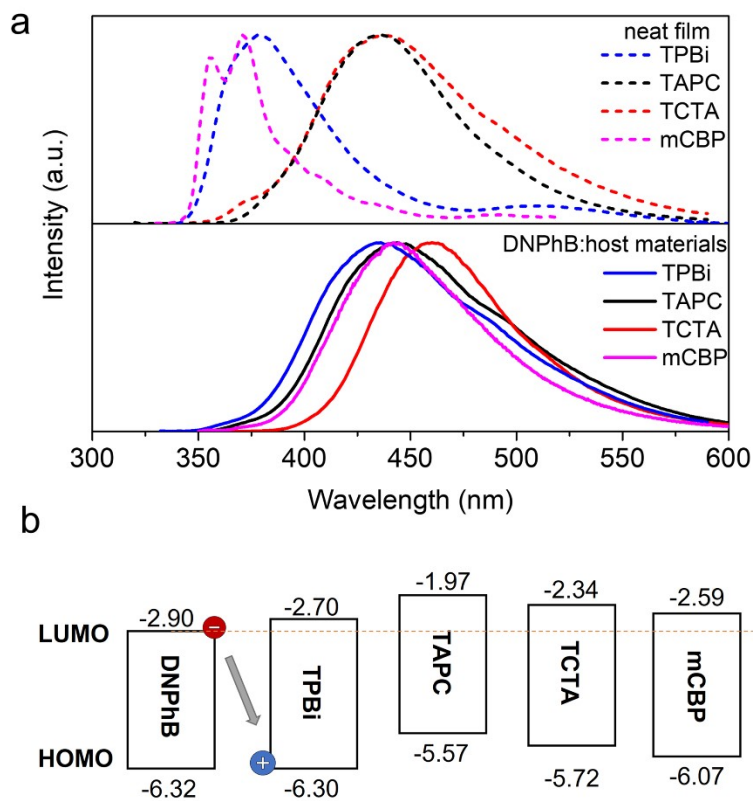
Fig. S5 (a) PL spectra of TAPC, TCTA, TPBi and mCBP neat films and 50% doped with DNPhB respectively. (b) HOMO and LUMO of DNPhB and the host materials.

Table S4. Photophysical properties of 50% doped with DNPhB respectively.

Host	$\lambda_{PL}{}^a$ (nm)	FHWH (nm)	$\Phi_{PL}{}^b$ (%)
TPBi	432	71	23.5
TAPC	448	70	10.5
TCTA	462	73	9.8
mCBP	444	71	53.6

[a] Steady-state PL at room temperature measured in films. [b] PL quantum yield measured in films using an integral sphere.
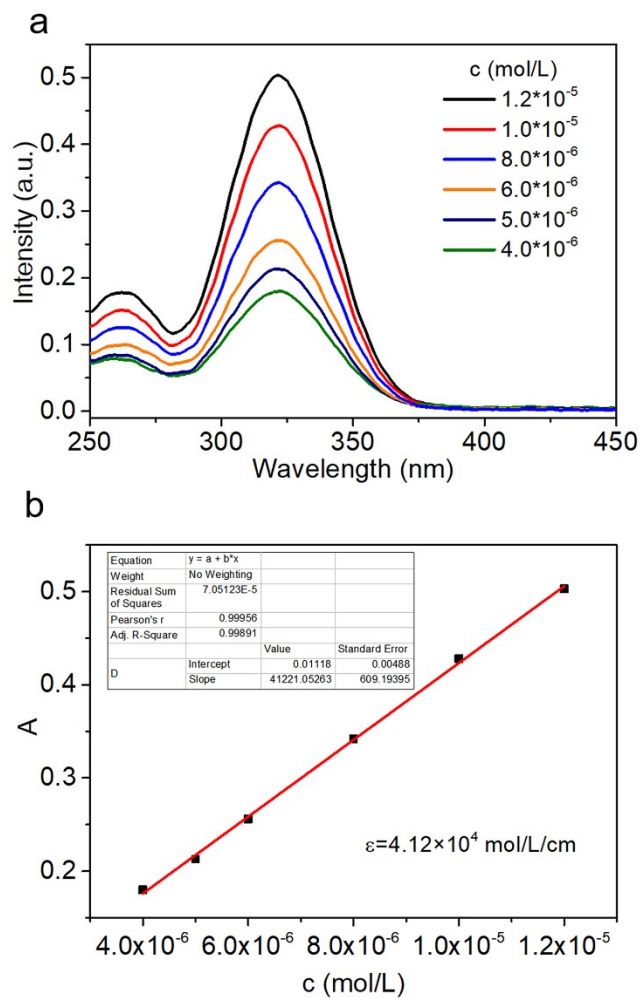
Fig. S6 Concentration dependence of the absorbance of DNPhB in THF at 330 nm.
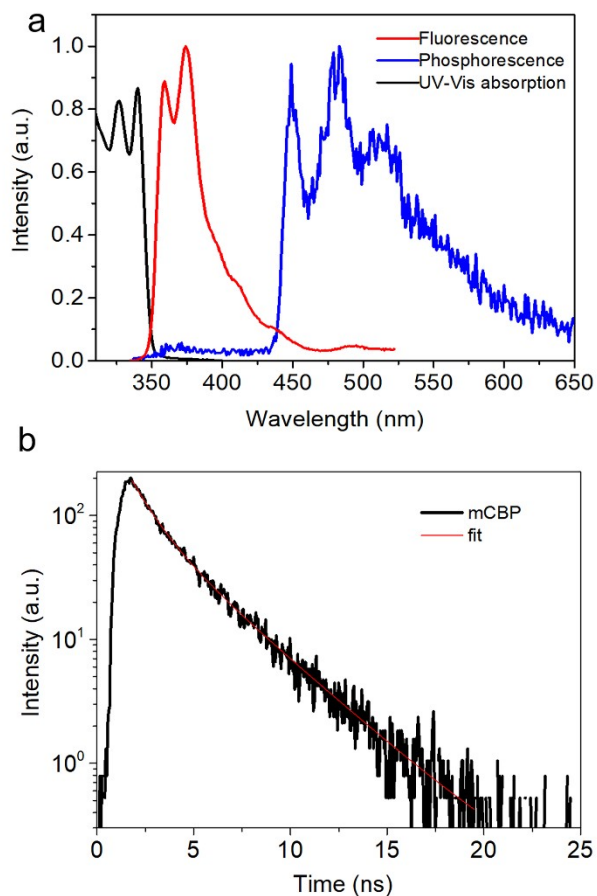
Fig. S7 UV-Vis absorption and PL spectra in pure films. (a) UV-Vis absorption and fluorescence spectra at room temperature and phosphorescence spectra at 77 K for mCBP. (b) PL transient decay spectra for neat films of mCBP at rt.

Table S5. Photophysical properties of mCBP in neat films.

Emitter	λ_{abs}[a] (nm)	λ_{PL}[b] (nm)	$\lambda_{Phos.}$[c] (nm)	E_g[d] (eV)	S_1[d] (eV)	T_1[d] (eV)	$\triangle E_{ST}$[d] (eV)	τ_p[e] (ns)
mCBP	347	370	455	3.48	3.56	2.85	0.71	0.64

[a] Absorption measured in 10^{-5} mol L^{-1} polystyrene solution; [b] Steady-state PL at room temperature measured in films; [c] Measured at 77 K with a delay; [d] Calculated from λ_{onset}; [e] Lifetime of fluorescence determined from the transient PL.
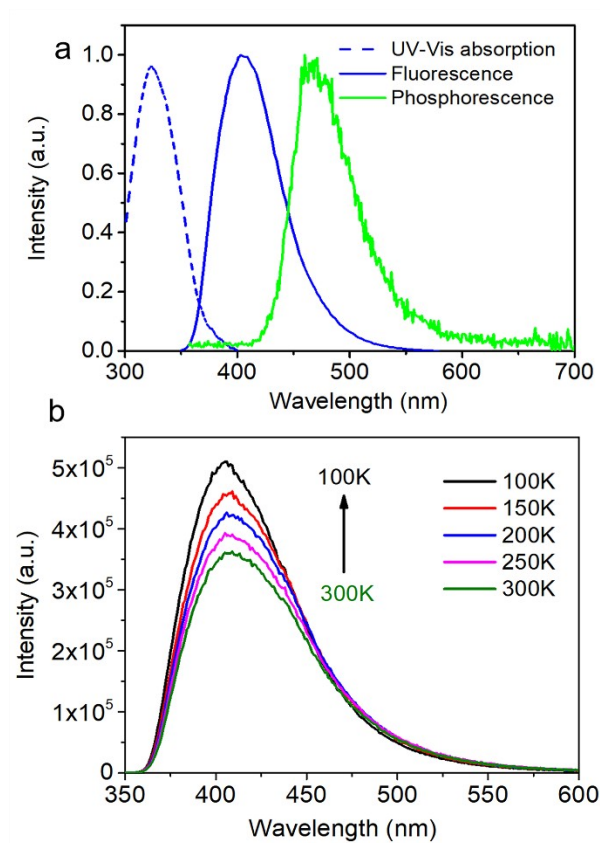
Fig. S8 UV-Vis absorption and PL spectra for neat films. (a) UV-Vis absorption and fluorescence spectra at room temperature spectra at 77 K for DNPhB. (b) PL spectra for DNPhB in films from 100 K to 300 K.
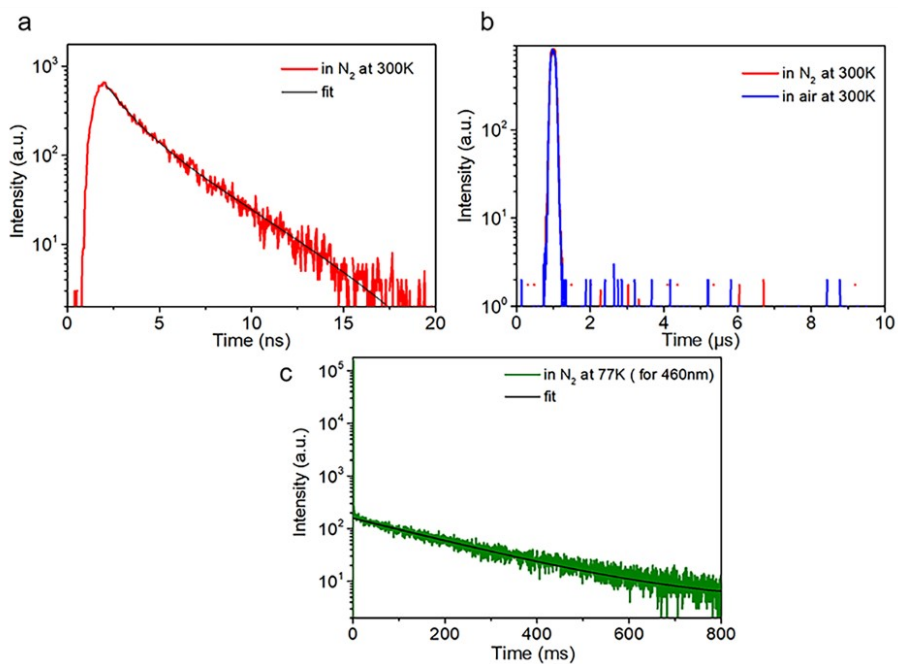
Fig. S9 PL transient decay spectra for neat films of (a), (b) DNPhB at rt.

Table S6. Photophysical properties for neat film of DNPhB.

Emitter	$\lambda_{abs}{}^{a}$ (nm)	$\lambda_{PL}{}^{b}$ (nm)	$\lambda_{Phos}{}^{c}$ (nm)	$E_g{}^{d}$ (eV)	$S_1{}^{d}$ (eV)	$T_1{}^{d}$ (eV)	$\triangle E_{ST}{}^{d}$ (eV)	$\tau_p{}^{e}$ (ns)
DNPhB	325	405	460	3.32	3.42	2.95	0.47	1.35

[a] Absorption measured in 10^{-5} mol L^{-1} Chlorobenzene solution. [b] Steady-state PL at room temperature measured in films. [c] Measured at 77 K with a delay. [d] Calculated from λ_{onset}. [e] Lifetime determined from the transient PL.

Note S1. Estimation of the Reverse intersystem crossing rate constant of the 50% MRs at 200K.
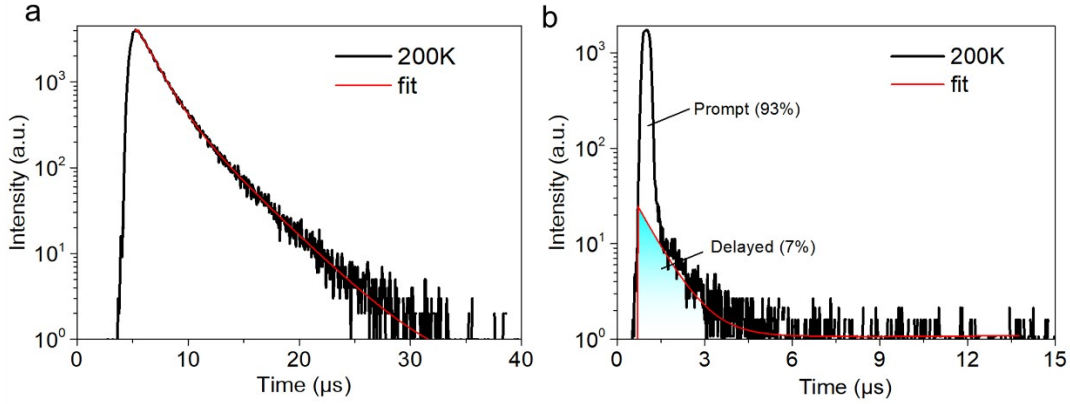
Fig. S10 Transient decay spectra of 50% DNPhB/mCBP at 200 K.

The values are determined from PLQY and the lifetimes of the fluorescence and TADF components. Φ_p and Φ_d are calculated by their ratios of the integral areas in the time-resolved spectrum. Both the prompt and delayed components exhibit biexponential decays, these can be attribute to the coexist of the monomer and dimer in the doping MRs, so τ_p and τ_d are the average lifetime of the prompt and delayed components, they are calculated by $\tau_{av} = \sum A_i \tau_i^2 / \sum A_i \tau_i$, where A_i is the pre-exponential for lifetime τ_i (A_i is the proportion of τ_i here). [1-3]

Φ=0.354

Φ_p=0.326

Φ_d=0.023

τ_p=1.16 ns

τ_d=0.85 μs

k_p=2.8*10^8

k_{IC}=5.2*10^8

k_{ISC}=5.8*10^7

Φ_{IC}=0.6

$$k_p = \emptyset_p / \tau_p \quad (1)$$

$$\emptyset = k_p / (k_p + k_{IC}) \quad (2)$$

$$\emptyset_p = k_p / (k_p + k_{IC} + k_{ISC}) \quad (3)$$

$$\emptyset_{IC} = k_{IC} / (k_p + k_{IC} + k_{ISC}) \quad (4)$$

Φ_{ISC}=0.067

$$\emptyset_{ISC} = k_{ISC}/(k_p + k_{IC} + k_{ISC}) \quad (5)$$

k_d=3.91*10^5

$$k_d = \emptyset_d/(\emptyset_{ISC} * \tau_d) \quad (6)$$

k_{RISC}=4.72*10^5

$$k_{RISC} = (k_p * k_d)/(k_p - k_{ISC}) \quad (7)$$

Then, k_{RISC} can be estimated from the experimentally observable rate constants and the PL quantum yield of the prompt and delayed components. If the intersystem crossing (ISC) is independent of temperature because the ISC process is considered as an adiabatic process, the k_{ISC} values at higher temperatures are set equal to that at 200 K.

Table S7. PL characteristics of the exciplex formed between mCBP and DNPhB versus temperature

T (K)	τ_p (ns)	τ_d (µs)	Φ_{total}	Φ_d	Φ_p
300	1.75	1.02 (20.8%)	54.0%	11%	43%
280	1.64	0.96 (17.8%)	50.0%	8.9%	41.1%
260	1.55	0.94 (13.0%)	47.2%	6.13%	41.1%
250	1.50	0.88 (11.0%)	45.0%	4.95%	40.1%
240	1.40	0.87 (9.23%)	43.0%	3.3%	39.7%
220	1.26	0.86 (8.51%)	38.7%	3.3%	35.4%
200	1.16	0.85 (7.0%)	35.0%	2.35%	32.6%

Table S8. Calculated rate constants of the exciplex emission from the mixed mCBP and DNPhB (molar ratio 1: 1) film.

T (K)	k_p ($10^8 s^{-1}$)	k_d ($10^5 s^{-1}$)	k_{ISC} ($10^8 s^{-1}$)	k_{RISC} ($10^5 s^{-1}$)
300	2.45	5.44	0.58	7.10
280	2.5	5.2	0.58	6.77
260	2.6	4.9	0.58	6.30
250	2.76	4.75	0.58	6.0
240	2.78	4.68	0.58	5.91
220	2.78	4.26	0.58	5.38
200	2.80	3.91	0.58	4.72
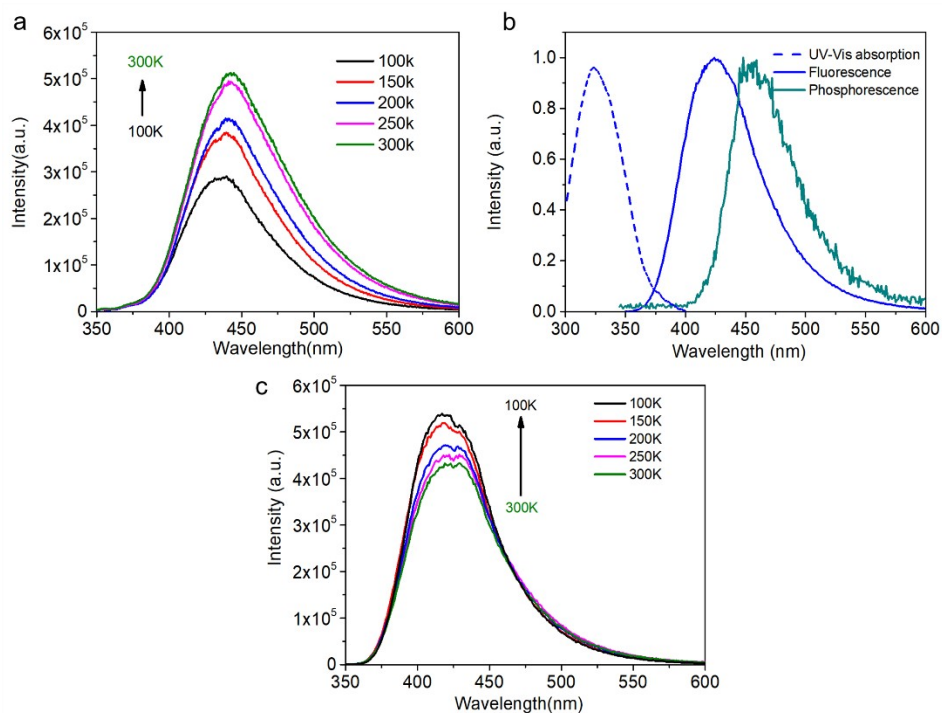
Fig. S11 **(**a) PL spectra for DNPhB (50%) in polystyrene films from 100 K to 300 K. (b) UV-Vis absorption and fluorescence spectra at room temperature and phosphorescence spectra at 77 K for DNPhB (50%) in polystyrene films. (c) PL spectra for DNPhB (50%) in polystyrene films from 100 K to 300 K.
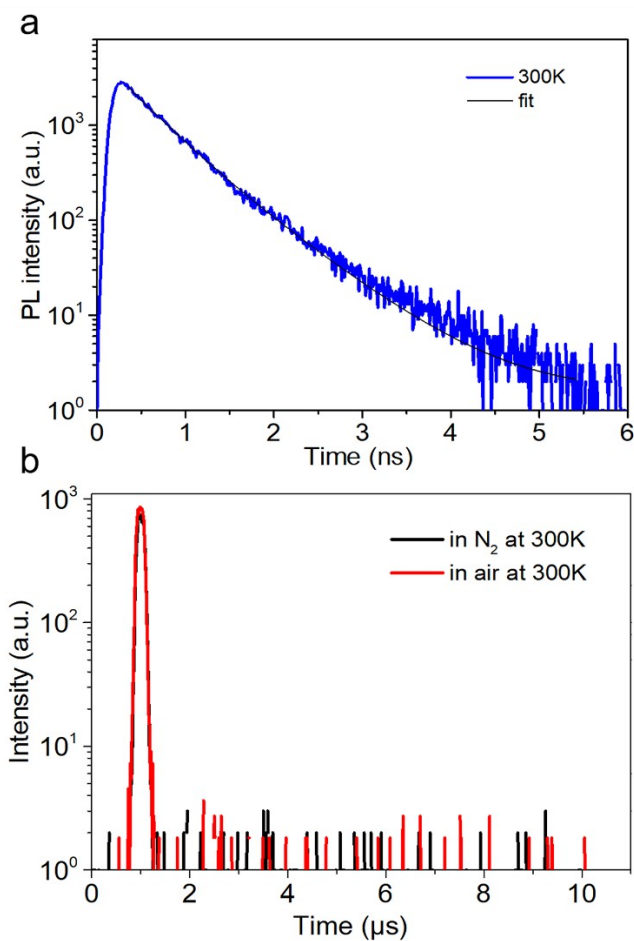
Fig. S12 PL transient decay spectra of (a) and (b) DNPhB in polystyrene films.

Table S9. Photophysical properties for polystyrene film of DNPhB.

Emitter	λ_{abs}[a] (nm)	λ_{PL}[b] (nm)	$\lambda_{Phos.}$[c] (nm)	E_g[d] (eV)	S_1[d] (eV)	T_1[d] (eV)	$\triangle E_{ST}$[d] (eV)	τ_p[e] (ns)	τ_p[e] (μs)
DNPhB	325	423	455	3.32	3.42	3.01	0.41	0.52	~

[a] Absorption measured in 10^{-5} mol L^{-1} polystyrene solution; [b] Steady-state PL at room temperature measured in films; [c] Measured at 77 K with a delay; [d] Calculated from λ_{onset}; [e] Lifetime of fluorescence determined from the transient PL.

Thermal Property Measurements

Thermogravimetric analysis (TGA) was conducted under a heating rate of 10ºC/min and a nitrogen flow rate of 50 cm³/min from 25ºC to 500ºC with a TG 209F3 Tarsus instrument. TGA reveals that DNPhB has a good thermal stability with a high decomposition temperature (T_d = 296ºC). Differential Scanning Calorimeter was conducted under a heating rate of 10ºC/min and a nitrogen flow rate of 50 cm³/min from 25ºC to 300ºC. Its glass transition temperature (T_g) is 353ºC, which is high T_g to ensure excellent film forming property after annealing.
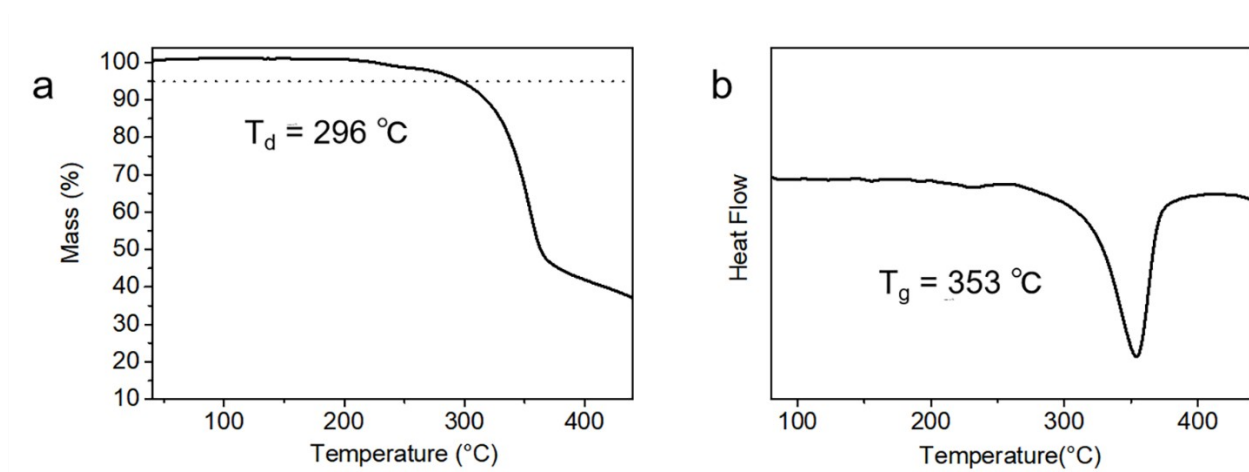
Fig. S13 Thermal gravimetric analysis (a) and differential scanning calorimetry analysis, (b) of DNPhB.

X-ray diffraction (XRD) Measurements

The X-ray diffraction (XRD) patterns were measured by a Smartlab 9KW X-ray diffractometer with Cu Kα radiation (λ= 1.54050 Å) operated in the 2θ range from 5° to 30°.
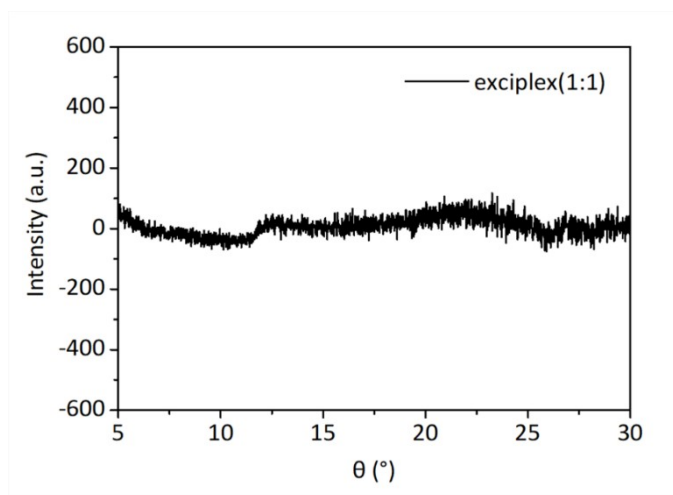
Fig. S14 XRD pattern of 1:1 vapor-deposited light-emitting layer with a thickness of 25 nm on ITO.

Atomic Force Microscopy (AFM) height images

The doping film morphology of mCBP:DNPhB was investigated by AFM measurements, which were carried out room temperature using a Bruker Dimension Icon AFM
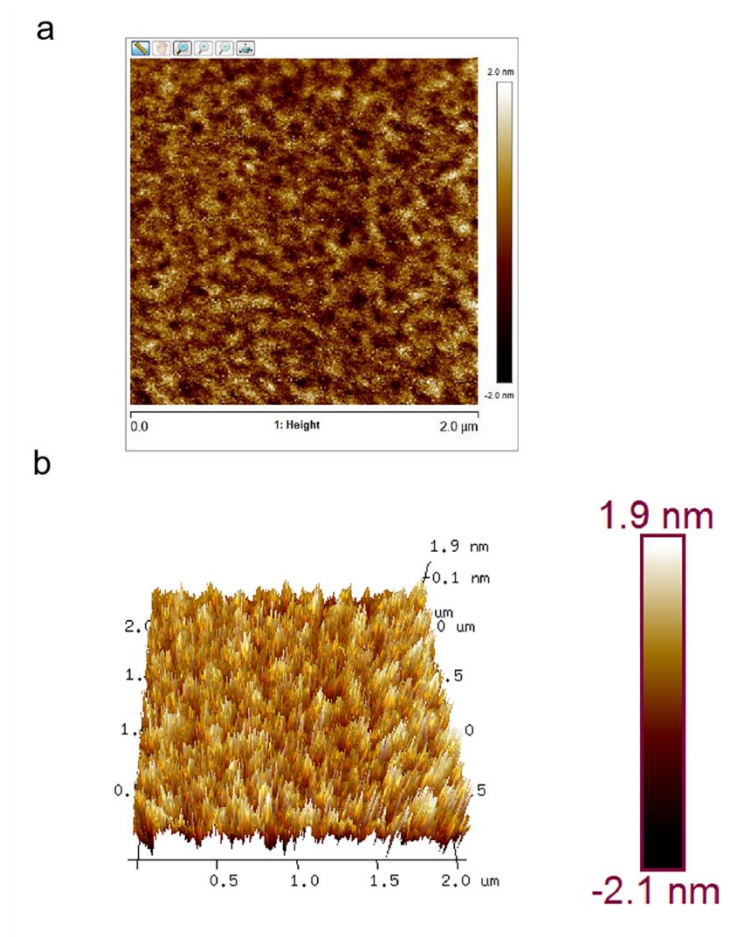
Fig. S15 AFM images (2 μm × 2 μm) of the surface morphology of the vacuum evaporated film (RMS = 0.65 nm) overlaid onto surface.

OLED Device Fabrication and Measurements

All the organic materials used directly in this OLED experiments (except for the DNPhB) were purchased from Xi'an Polymer Light Technology Corp. The ITO substrates were firstly cleaned with isopropyl alcohol and deionized water, then dried in an oven at 110 °C, treated with O_3 plasma. After that, the samples were transferred to a thermal evaporator chamber. Organic materials, LiF, and Al were deposited by thermal evaporation under a pressure of 2×10^{-4} Pa. The electroluminescence characters were measured with a Photoresearch SpectraScan PR735 spectrometer and the current-voltage characteristics were measured using Keithley 2400 source meter under the encapsulation conditions.
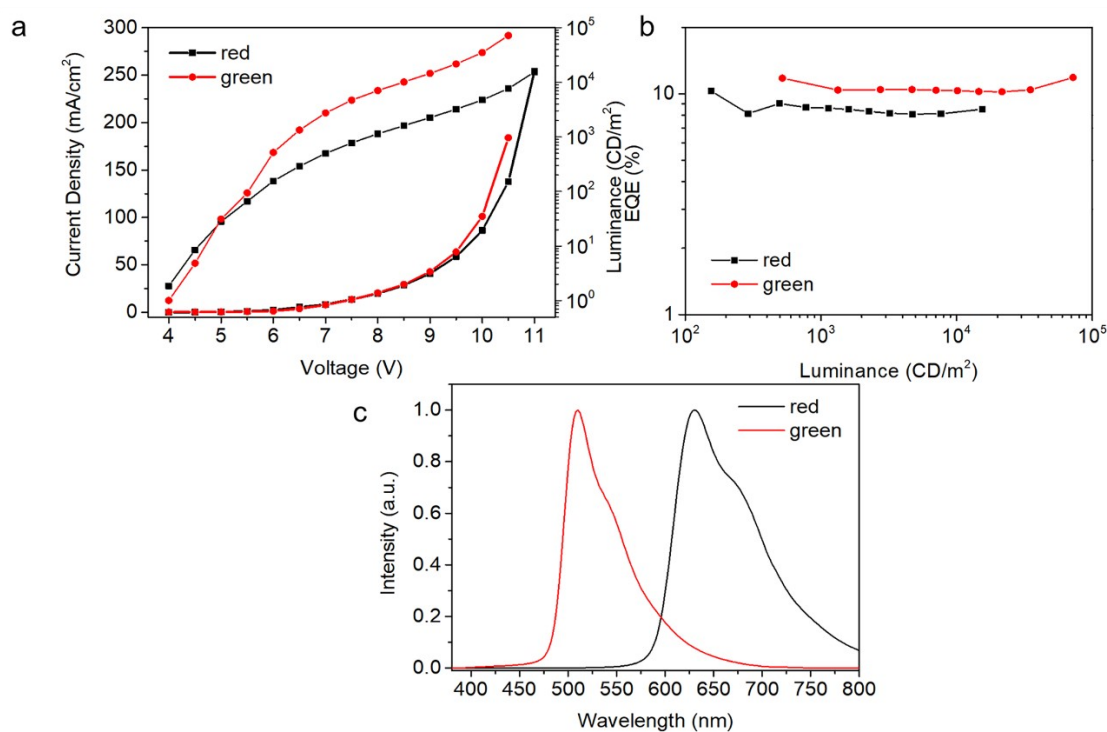
Fig. S16 OLED properties of the different doped in traditional host materials (mCBP). (a) The current density-voltage-luminance curves of the devices. (b) External quantum efficiency versus luminance. (c) Electroluminescent (EL) spectra in 1000 cd m^{-2}.

Table S10. The summary of the deep-blue devices performances.

Device	$V_{on}{}^{a}$ (V)	L_{max} (cd m^{-2})	CE/PE/EQE^{b} (cd A^{-1}/lm W^{-1}/%)		Peak$_{max}{}^{c}$ (nm)	CIE^{c} (x, y)
			Maximum	At 1000 cd m^{-2}		
40%	3.7	4098	2.63/2.07/4.26	2.26/1.02/3.46	444	（0.152, 0.079)
50%	3.7	5486	3.04/2.20/4.83	2.65/1.28/4.24	444	（0.152, 0.075)
60%	4.0	5001	3.07/2.11/4.06	2.64/1.10/3.54	450	（0.152, 0.090)

^{a} The voltage at the luminance of 1 cd m^{-2}; ^{b} CE: current efficiency; PE: power efficiency; EQE: external quantum efficiency; ^{c} CIE coordinates measured at 1000 cd m^{-2}.
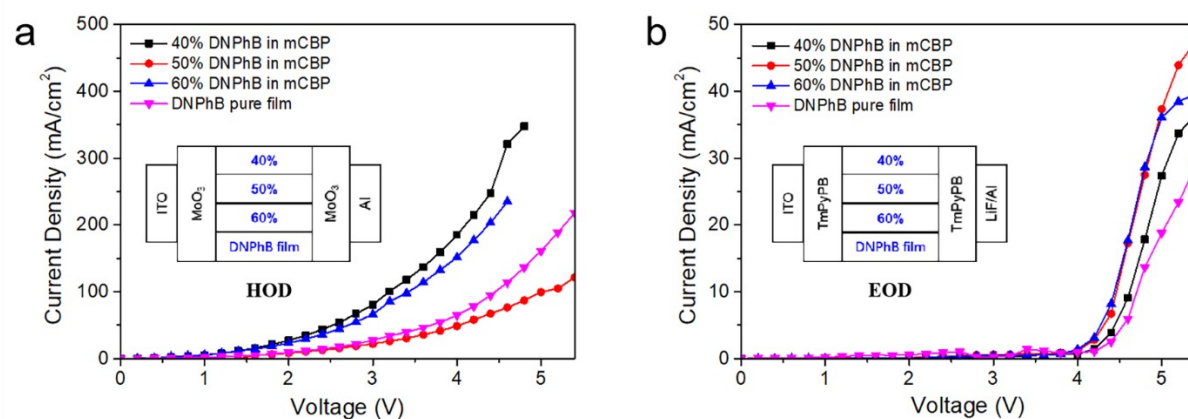
Fig. S17 The J-V curves for both hole-only device (HOD) and electron-only device (EOD). The HOD structure consists of ITO/MoO$_3$(10nm)/EML(50nm)/MoO$_3$(10nm)/Al(100nm), while the EOD structure comprises ITO/TmPyPB(10nm)/EML(50nm)/TmPyPB(10nm)/ LiF(1nm)/ Al(100nm). The inset in (a) and (b) respectively shows the device structures for HOD and EOD.
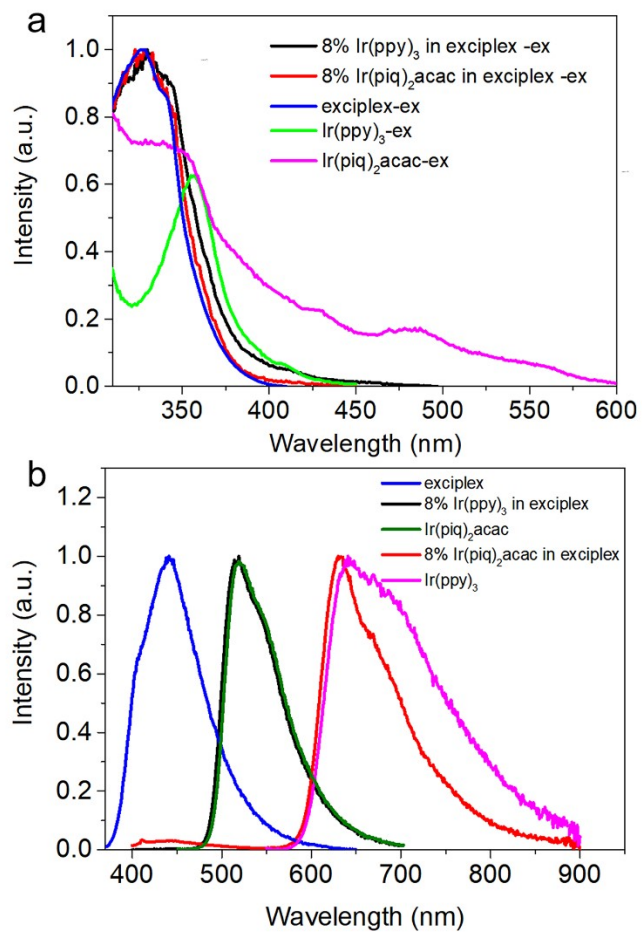
Fig. S18 (a) Excitation spectra and (b) PL spectra for 8% Ir(ppy)$_3$/8% Ir(piq)$_2$acac in exciplex, exciplex, Ir(ppy)$_3$, Ir(piq)$_2$acac films at 300 K.

References

1. Q. S. Zhang, H. Kuwabara, W. J. Potscavage, S. P. Huang, Y. Hatae, T. Shibata and C. Adachi, Journal of the American Chemical Society 2014, **136**, 18070.
2. X. Y. Cai, W. D. Qiu, M. K. Li, B. B. Li, Z. H. Wang, X. Wu, D. C. Chen, X. F. Iang, Y. Cao and S. J. Su, Advanced Optical Materials 2019, **7**, 1801554
3. R. B. Bai, X. W. Meng, X. X. Wang and L. He, Advanced Functional Materials 2021, **31**, 2007167